

# On the growth of massive scalar hair around a Schwarzschild black hole

Katy Clough,<sup>1,\*</sup> Pedro G. Ferreira,<sup>1,†</sup> and Macarena Lagos<sup>2,‡</sup>

<sup>1</sup>*Astrophysics, University of Oxford, DWB, Keble Road, Oxford OX1 3RH, UK*

<sup>2</sup>*Kavli Institute for Cosmological Physics, The University of Chicago, Chicago, IL 60637, USA*

(Dated: Received January 24, 2023; published – 00, 0000)

A broad range of theories of gravity lead to no-hair theorems: even in the presence of extra fields which are non-minimally coupled to gravity, black holes are exactly as those found in General Relativity. We show that it is possible to grow hair on a what was originally a (no-hair) Schwarzschild black hole if one assumes a periodically time-varying (but spatially homogeneous) background for the extra field. Through numerical simulations of a minimally coupled massive Klein-Gordon scalar field, we show how a non-trivial profile can emerge on a time scale related to the mass of the black hole. We undertake simulations with and without backreaction on the metric and see that the essential, qualitative features remain consistent. The results are particularly relevant for scalar-tensor theories of gravity and dark matter models consisting of a massive scalar, e.g. axions.

**Introduction:** Black holes (BHs) are some of the most remarkable objects in nature. While we have acknowledged their existence for many decades, the recent detections of BH mergers by Advanced LIGO [1] and VIRGO [2], or the imaging of the event horizon of the BH at the heart of M87 [3], further reinforce our belief in them as a part of the astronomical zoo. BHs are also remarkably featureless. In the context of GR and under certain restrictive assumptions [4, 5], it is often stated that BHs have *no hair*. This is true even for a broad class of extensions of GR [6–9]. Yet, BHs live in a dynamical, complex and evolving Universe which breaks many of these assumptions and so, given our new-found ability to probe BHs with gravitational waves or imaging, one needs to revisit the possibility that they may have hair.

Of particular interest is the possibility that a BH may have scalar hair [10]. This means that it will have a scalar field  $\phi$  with a non trivial profile surrounding it which may, in turn, modify the metric. Scalar fields exist in nature, can arise in a number of candidate fundamental theories [11], and may lead to “fifth” forces which can be constrained in a number of ways [12]. They are also the basis for several popular dark matter (DM) candidates, such as axions. A number of counterexamples violating the no hair theorems have been analyzed, leading to either long lasting hair or wigs [13–15]. Furthermore, in the case of rotating – i.e. Kerr – BHs, a superradiant instability can lead to the spontaneous production of scalar particles, without requiring an initial seed (see [16] for a review). In this Letter, we discuss the scenario where scalar hair grows due to the fact that the BH and scalar field are embedded in a time varying but spatially homogeneous background (such as in the case of the axion).

In a seminal paper [17], Jacobson showed that it was possible to endow a BH with hair if it is embedded in a cosmological spacetime dominated by a minimally-coupled massless scalar field. Specifically, he considered a Schwarzschild background with spacetime line element:

$$ds^2 = -f(r)dt^2 + f^{-1}(r)dr^2 + r^2(d\theta^2 + \sin^2\theta d\phi^2), \quad (1)$$

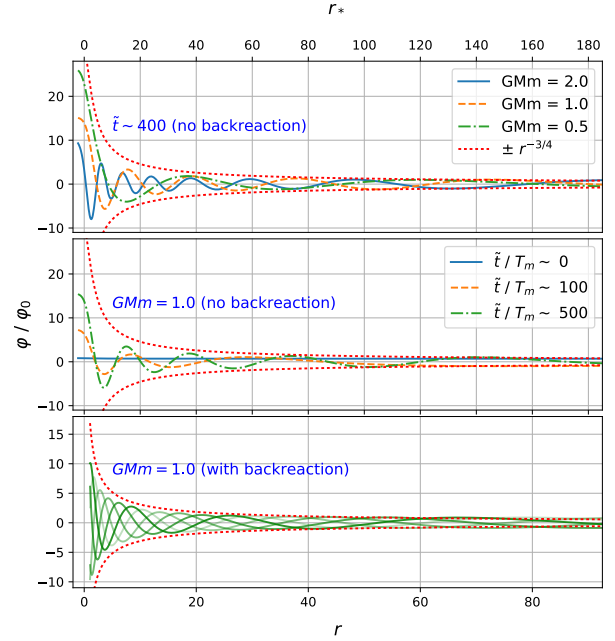


FIG. 1. Two top figures show  $\phi$  as a function of  $r_*$  without backreaction. The first plot shows that the profiles depend on mass in a similar way to the expected analytical profiles – i.e. there are more oscillations for higher masses, and the envelope of the oscillations is well fit at larger radii by  $r^{-3/4}$ . The second illustrates the growth in time of the amplitude from a homogeneous state (with  $T_m = 2\pi/m$ ). The bottom plot shows a timelapse of  $\phi$  versus  $r$  over a period of oscillation at a time of  $\tilde{t}/T_m \sim 200$  for the backreacting case, which shows a consistent build up and profile.

where  $t$ ,  $r$ ,  $\theta$  and  $\phi$  are the time and polar coordinates,  $f(r) = 1 - \frac{R_s}{r}$  with  $R_s = 2GM$  being the Schwarzschild radius in terms of the mass of the BH  $M$  and Newton’s constant  $G$ . He showed that in this background it was possible to construct a non-trivial solution for  $\phi(t, r)$  which varied with time asymptotically,  $\phi(t, r \rightarrow \infty) \propto t$  and which was regular at the horizon.

In this Letter, motivated by Jacobson’s work, we focus on the case of a minimally-coupled scalar field with mass  $m$  and analyze the dynamical formation of scalar hair around a Schwarzschild BH. In particular, we numerically study and show how an initially homogeneous and isotropic cosmolog-

\* katy.clough@physics.ox.ac.uk

† pedro.ferreira@physics.ox.ac.uk

‡ mlagos@kicp.uchicago.edu

ical scalar field, with  $\varphi(t) \propto e^{imt}$ , evolves in time and settles around the BH, forming a scalar cloud (illustrated in Fig. 1).

**Framework:** Consider a single real scalar field minimally coupled to the metric, satisfying the massive Klein-Gordon equation on a curved spacetime. Let us assume that the energy density of the scalar field is low enough that we can neglect backreaction of the metric and consider the spacetime to be given by the Schwarzschild background in eq. (1) (we consider the effect of backreaction later). Such scalar field can arise, for example, in scalar-tensor theories [18, 19], or as a good approximation to an axion-like particle with mass  $m$  [20–23].

The equation of motion of the scalar field for spherically-symmetric profiles will be given by the Regge-Wheeler equation [24, 25]:

$$\left[ \frac{\partial^2}{\partial t^2} - \frac{\partial^2}{\partial r_*^2} + V_s(r) \right] \varphi(t, r) = 0, \quad (2)$$

with  $r_* = r + R_S \ln(r/R_S - 1)$  the tortoise coordinate and  $V_s(r) = f(r) (R_S/r^3 + m^2)$  the effective potential, for the relevant case of zero angular momentum. One can look for solutions of the form  $\varphi = e^{i\omega t} \psi(r)$ , and see that near the event horizon ( $r \rightarrow R_S$ ) we have that  $V_s \approx 0$  and the solutions are superpositions of ingoing waves,  $\varphi \propto e^{i\omega(t+r_*)}$ . Conversely, at spatial infinity we have  $V_s \approx m^2 f(r)$  and the solutions are such that  $\varphi \propto e^{im(t \pm 2\sqrt{r_*})} / r^{3/4}$  for  $\omega = m$  or  $\varphi \propto e^{i(\omega t \pm k r_*)} / r$  for  $\omega^2 = m^2 + k^2$ . It is possible to construct exact solutions (which we will not study here) for the entire spacetime [26–29], based on the Huen functions which describe a scalar cloud surrounding the BH and smoothly interpolate between the two regimes mentioned above<sup>1</sup>. For a thorough analysis of the scalar field cloud in this case, see [30]. In this letter we focus on the dynamical growth of hair from a completely homogeneous scalar field to the scalar cloud described. This is somewhat different to the analytic solutions as we do not require that the spatial profile decays at infinity, but rather consider a cosmological setup in which the field has an asymptotically finite amplitude of oscillation, at least over some region which is large relative to  $R_S$ .

For cases without backreaction, we employ the code and methods of [31]. We fix the metric to eq. (1), although we use Cartesian Kerr-Schild coordinates (see e.g. [32]), which are horizon penetrating. The Kerr-Schild time coordinate  $\tilde{t}$  is related to the Schwarzschild coordinate  $t$  through  $\tilde{t} = t + R_S \ln(r/R_S - 1)$ . The radial coordinates are those of Schwarzschild but in presenting our results we convert to the tortoise coordinate  $r_*$  for clarity. We set  $R_S = 1$  and study the formation of the cloud in three different cases:  $GMm = 0.5$ ,  $GMm = 1$ ,  $GMm = 2$ .

For cases with backreaction, the numerical relativity code GRCHOMBO ([www.grchombo.org](http://www.grchombo.org)) is used (see [33, 34] for details). The approach and code was adapted from that used in [35], which employed standard Numerical Relativity

(NR) techniques. The BSSN/CCZ4 formulation of the Einstein Equations is combined with the moving puncture method for stable evolution of BH spacetimes, and the initial data is conformally flat Bowen-York data [36] for an isolated BH. We are required to add a spatially constant value for the trace of the extrinsic curvature,  $K = -\sqrt{24\pi\rho_0}$ , so that the Hamiltonian constraint is properly satisfied in the presence of the non-zero field. This results in a background with the spacetime asymptotically expanding, as motivated by our cosmological scenario. For these simulations we focus on the case with  $GMm = 1$ .

For all simulations the initial conditions for the scalar field are set to  $\varphi(t=0, r) = \varphi_0$  and  $\partial_t \varphi(t=0, r) = 0$ . We choose an initial amplitude  $\varphi_0$  such that the energy density is  $\rho(t=0, r) = \rho_0 = 10^{-10} R_S^{-2}$  in geometric code units. In physical units this is *significantly* higher than the average energy density of dark matter<sup>2</sup>. In the case without backreaction, we are only interested in the evolution of the field and the absolute energy density of the field is not particularly relevant, but in the case with backreaction we should bear in mind that the expansion of spacetime and backreaction effects will be significantly higher than in a physically realistic scenario, so this is an overly stringent test of robustness to backreaction effects.

We implemented non-zero, time oscillating boundary conditions for the scalar field by extrapolating the field from within the numerical domain. After testing several possibilities, we imposed that the field amplitude is extrapolated either linearly  $\varphi = B - Ar$  or as  $r^{-3/4}$  at the boundaries, with the case chosen at each step which minimises the change from the values within the domain. During the build up of the cloud the energy density at the boundaries decreases only fractionally and the field profile remains smooth as it oscillates. Note that, unlike in the analytic solution, our boundaries do not permit ingoing waves of frequency  $m$ , and are not initially constrained to decay as  $r^{-3/4}$ . Despite this, we see the growth of a cloud with a similar form to the analytic solutions.

**Results:** We begin with the results without backreaction. In Fig. 1 we see the growth of the scalar amplitude around the BH for  $GMm = 1$ , starting from a homogeneous profile; after an initial transient period, there is a steady, approximately linear build up in the ingoing waves, which have a spatial envelope well fit by a  $1/r^{3/4}$  dependence. Note that further out the field asymptotes to a homogeneous profile (the boundary is at  $r = 512R_S$ ), so an extrapolation of the  $1/r^{3/4}$  fit at smaller  $r$  lies above the asymptotic values. Over time the amplitude at the boundary is decreasing – the field is gradually redistributing itself into the analytic profile – but the timescale for this is longer than the simulation time. We show the time evolution in more detail in Fig. 2, which shows the evolution of the amplitude of the scalar field oscillations as a function of time at several selected values of  $r_*$ .

<sup>1</sup> Note that these solutions are fundamentally different to the bound states which are excited by superradiant growth.

<sup>2</sup>  $10^{-10} R_S^{-2}$  is between  $\sim 10^{30}$  greater than the DM density in the case of solar mass BHs (which is equivalent to the density of a white dwarf star) and  $\sim 10^{10}$  times greater for SMBHs like that of M87, equivalent to a density of  $10^{-10} \text{ kg/m}^3$ . Note that similarly unrealistic values are sometimes used in evolving Neutron Star binaries in a non zero atmosphere.

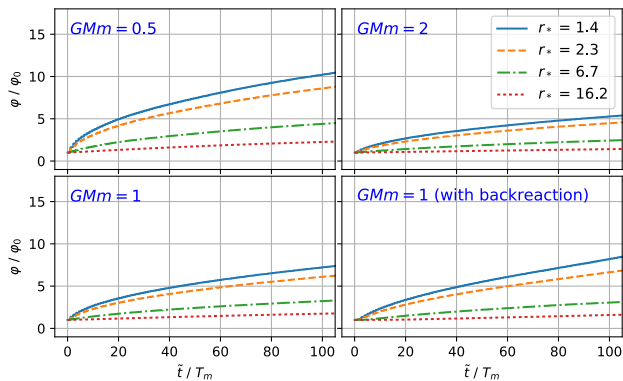


FIG. 2. The amplitude of the oscillations in  $\phi$  as a function of the number of oscillations  $T_m = 2\pi/m$  for various radii and values of  $GMm$  as labelled. The bottom right figure shows the case of  $GMm = 1.0$  with backreaction included. Note that in the backreaction case we cannot define  $r_*$  as the gauge is dynamical, but we select the same coordinate locations as the fixed case for the plot. Whilst these will not give the same physical positions in space, we still see a consistent pattern for the build up.

The rate of growth is faster as a function of the number of oscillations,  $n$ , in the lower mass cases, with a dependence on  $m$  after the initial transient period of  $\frac{1}{\phi_0} d\phi/dn \propto 1/\sqrt{m}$ . Given that the oscillation period  $T_m \propto 1/m$ , the physical rate of build up will scale as  $\frac{1}{\phi_0} d\phi/dt \propto \sqrt{m}$ .

The top panel of Fig. 3 shows the volume integral of the energy density within a radius of  $r = 100R_s$  (excluding the region within the horizon), with  $\frac{1}{\int \rho_0 dV} d(\int \rho dV)/dn \propto 1/m$  as expected since the energy density scales as  $\rho \propto \phi^2$ . Thus the energy density grows at a rate in real time which is independent of the mass of the field, and we measure the physical time for the mass within  $r < 100R_s$  to double as  $t = (M/M_\odot)6$  ms. These values are consistent with the freefall timescale for the BH, which is reasonable as the oscillating scalar should behave roughly as matter for  $GMm > 1$ , and our initial conditions do not provide it with angular momentum for support. However, unlike a true pressureless dust, the scalar does not fall into the BH but rather builds up in a cloud, supported by the scalar gradients. Previous results have shown that the decay rate of scalars around BHs is small, so that they do not need significant energy input to grow. The growth rate of the cloud is thus approximately independent of the mass of the scalar<sup>3</sup>.

The bottom panel of Fig. 3 shows the energy flux across spheres of radius  $r_*$ , calculated as  $dE/dt = 4\pi r^2 S_r$  with the momentum density  $S_r(r) \propto \partial_r \phi \partial_t \phi$ . The values are averaged over several oscillations of the field, showing a net inflow towards the BH (note that the momentum density actually oscillates between inflow and outflow over each period). At later times the flux at larger radii appears to level out into a constant inflow, but the rate of inflow at smaller radii is relatively

suppressed, which results in the growth of the cloud as shown in the top panel of the figure.

In the case of  $GMm = 1$  it appears that the cloud saturates at a constant energy density around  $\tilde{t} \sim 700T_m$ . However, we found that at later times the field oscillations became disturbed, with large oscillations in the amplitudes. This is most likely due to unphysical effects from the imposed boundaries. The  $GMm = 0.5$  case appears to grow further, and did not saturate in the time studied. This requires further investigation, but notice in Fig. 1 that the spatial oscillations and  $r^{-3/4}$  profile spread outwards from the BH as time elapses. At some point the boundary condition imposed starts to be inconsistent with the physical solution, in which the oscillations would continue to spread outwards throughout the homogeneous field. We therefore expect that the cloud should continue to grow in accordance with the freefall timescales, feeding off the reservoir at  $r = +\infty$ . As we explain in the discussion section, these timescales may be cosmological for physical DM systems.

During the growth of the scalar cloud the time frequency of the oscillations depends on time and space, but after only  $\sim 20$  oscillations it converges to a constant given by  $m$ . We observe a similar behaviour for the spatial frequencies, with a spatial dependence on  $m$  as shown in Fig. 1. Our results thus approximately fit the  $k = 0$  analytical results, which is consistent with our choice of initial conditions – set such that the spatial momentum of the field is zero. This is consistent with the cold DM case, for which the momentum is small relative to the mass, although one would expect a non zero angular momentum.

We now focus on the case with backreaction. The plots in Fig. 1 and Fig. 2 compare the profiles and evolution of the scalar field as a function of time in the backreacting and non-

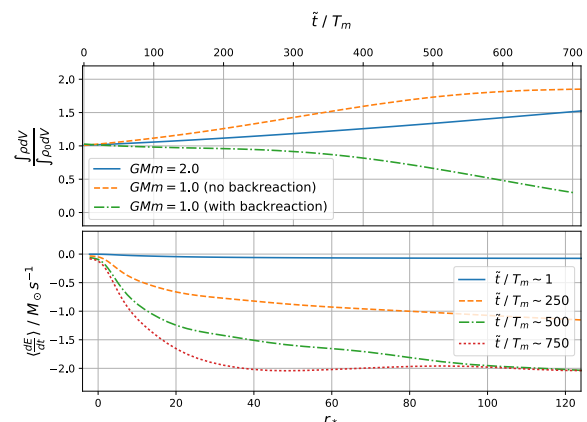


FIG. 3. The top panel shows the volume integral of  $\rho$  within a radius  $r = 100R_s$  (excluding the region within the horizon) as a function of  $T_m = 2\pi/m$ . In the backreaction case an energy decrease is observed due to the effect of the cosmological expansion, but the other cases consistently show a growth. The bottom panel shows the energy flux  $dE/dt$  across spheres of radius  $r_*$ , averaged over several periods, for the case  $GMm = 1$  without backreaction. Note that the relatively high flux values are the result of the large value of  $\rho_0$  used in our simulations, and one would expect the actual rates to scale with  $\rho_0$  accordingly.

<sup>3</sup> Note that this will not be the case for smaller values of  $GMm < 1$ , where the analytic solutions change to standing waves and the timescales may depend on  $m$ .

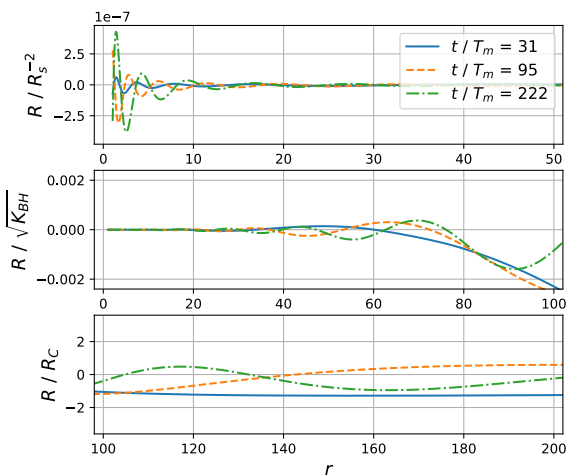


FIG. 4. Plot showing the 4D Ricci scalar  ${}^{(4)}R$  in absolute terms in units of  $R_s^{-2}$  (top), relative to the scale of curvature of the BH  $\sqrt{K_{BH}}$  at small radii (middle) and relative to the Ricci scalar for the asymptotic cosmological spacetime  $R_C$  at larger radii (bottom). Whilst the effects close to the BH are small relative to the curvature of the BH itself, further out the deviations become more significant.

backreacting case. Whilst in the backreacting case the dynamical gauge means that the field cannot be directly compared at the same radial coordinate, the two do show a very similar rate of build up, meaning that, at least in the initial stages, backreaction does not suppress the growth of the cloud.

Whilst the build up shows roughly the same growth in the amplitude at a given coordinate radius in the backreacting case as at a fixed tortoise coordinate  $r_*$  in the non-backreacting one, in the former the energy density of the cloud is actually being diluted by the expansion of the spacetime as the average scale factor increases by about 10%. As illustrated in the top panel of Fig. 3, the overall energy of the cloud within a radius  $r = 100R_s$  thus decreases over time. This illustrates that, depending on the asymptotic energy density of the field, the dilution due to expansion may out-compete the growth of the cloud. Assuming that the energy density of the cloud will scale as radiation, rather than matter (due to the significant contribution of the gradients), the critical value for the energy density at which the initial rate of dilution equals the rate of accumulation of the cloud is  $\sim 10^{-12}R_s^{-2}$ , a factor of 100 smaller than the value we used, but still orders of magnitude larger than most physically relevant values, such as those in DM halos. We thus conclude that the backreaction of the scalar on the metric and the effects of cosmological expansion should not disturb the build up significantly in realistic scenarios.

In Fig. 4 we quantify the non-zero value of the 4D Ricci scalar as a result of the presence of the cloud, calculated as  ${}^{(4)}R = 8\pi(\rho - S)$  with  $S$  the isotropic stress of the scalar field. The absolute values are compared to the square root of the Kretschmann Scalar for the BH  $K_{BH} = 12R_s^2/r^6$  and the Ricci scalar for the cosmological spacetime  $R_C = 24\pi G\rho_0$ . Whilst the effects close to the BH are small relative to the curvature of the BH itself, further out the deviations become more sig-

nificant, and asymptote to values of order  $R_C$ , but with a characteristic oscillating imprint related to the mass of the scalar.

*Discussion:* We have shown how massive scalar hair can emerge in a dynamical situation, with non-trivial time-varying boundary conditions set by cosmology. The scalar hair grows even in simulations in which backreaction from the metric is taken into account, stabilizing into a scalar field cloud. The growth timescales of the cloud are comparable to the freefall timescales for the BH, with the scalar cloud feeding off the (in principle infinite) reservoir at  $r = +\infty$ . Including backreaction, we find that the scalar field profile evolution is very similar, only diluted by the cosmological expansion for the values chosen – for more realistic values this effect would be small. We find a profile of oscillating deviations to the Ricci scalar with a scale set by  $m$ , which propagate outwards from the BH over time.

To approximately illustrate the potential cloud sizes, consider the example cases of a solar mass BH in a background of DM with a density  $\sim M_\odot/\text{pc}^3$  and a homogeneously oscillating region of size  $L \sim \text{pc}$ , or a SMBH with a mass of  $10^{10}M_\odot$  in a region of size  $L \sim \text{kpc}$ . In thinking about an end state, we are implicitly assuming that the region is just some local homogeneous patch, rather than a field which is truly stretching out to infinity. In the former case the matter should simply redistribute from a uniform distribution into a  $r^{-3/2}$  profile for the energy density, such that the oscillations at the boundary ultimately decay to zero in a time related to the freefall time  $t_{ff} \sim \left(\frac{L}{R_s}\right)^{3/2} R_s$ . In the latter case, the build up will spread outwards from the BH but can never saturate as the reservoir of scalar matter is infinite as  $r \rightarrow \infty$  and cannot be depleted (although the Hubble scale ultimately provides a finite limit). Assuming the former, we can quantify the time to reach a final state as  $\sim 10$  million years for the solar mass BH and  $\sim 1$  million years for the SMBH, with  $\rho$  at the horizon ultimately enhanced by a factor of  $10^{19}$  and  $10^9$  respectively, assuming that the scalar mass is conserved and does not fall into the BH.

We emphasise that our discussion neglects angular momentum, which would reduce the infall and change the picture for a more physically realistic scenario. But we would still expect similar clouds to build up, only with an angular spatial dependence in the profile related to the relevant spherical harmonics.

One may also consider a non-DM cosmological scalar – for example, a scalar that is part of a modified gravity model. Even very tiny coherent oscillations, on cosmological scales, would build up in amplitude around BHs in a similar way to what we describe here, leading to modifications to GR localised around BHs which increase over time.

With new windows on the Universe – gravitational waves and the EHT – we are probing BHs in ever more dynamical situations. Our hope is that the process we describe here will be further enriched in binary BH systems. There is already tentative evidence that a cloud of axions around inspiralling BHs will impact on the merger [37–39]. But one also expects cases where binary systems have time scales similar to that of the scalar field to show interesting behaviour (see [40–42]). We are currently exploring this dynamical pathway.

## ACKNOWLEDGMENTS

We thank Vitor Cardoso for his comments on an initial draft, and the authors of [30] for sharing details of their work. PGF acknowledges support from STFC, the Beecroft Trust and the European Research Council. ML was supported by the Kavli Institute for Cosmological Physics at the University of Chicago through an endowment from the Kavli Foundation and its founder Fred Kavli. KC is supported by the European Research Council. She thanks her GRChombo collaborators and acknowledges useful conversations with J Aurrekoetxea, T Helfer, EA Lim, M Radia and H Witek.

The simulations presented in this paper used the Glamdring cluster, Astrophysics, Oxford, and DiRAC resources under the projects ACLP151 and ACSP191. This work was per-

formed using the Cambridge Service for Data Driven Discovery (CSD3), part of which is operated by the University of Cambridge Research Computing on behalf of the STFC DiRAC HPC Facility ([www.dirac.ac.uk](http://www.dirac.ac.uk)). The DiRAC component of CSD3 was funded by BEIS capital funding via STFC capital grants ST/P002307/1 and ST/R002452/1 and STFC operations grant ST/R00689X/1. The work also used the DiRAC@Durham facility managed by the Institute for Computational Cosmology on behalf of the STFC DiRAC HPC Facility ([www.dirac.ac.uk](http://www.dirac.ac.uk)). The equipment was funded by BEIS capital funding via STFC capital grants ST/P002293/1 and ST/R002371/1, Durham University and STFC operations grant ST/R000832/1. DiRAC is part of the National e-Infrastructure.

- 
- [1] LIGO Scientific Collaboration, J. Aasi, B. P. Abbott, R. Abbott, T. Abbott, M. R. Abernathy, K. Ackley, C. Adams, T. Adams, P. Addesso, and et al., *Classical and Quantum Gravity* **32**, 074001 (2015), arXiv:1411.4547 [gr-qc].
- [2] F. Acernese, M. Agathos, K. Agatsuma, D. Aisa, N. Allemandou, A. Allocca, J. Amarni, P. Astone, G. Balestri, G. Ballardin, and et al., *Classical and Quantum Gravity* **32**, 024001 (2015), arXiv:1408.3978 [gr-qc].
- [3] Event Horizon Telescope Collaboration, K. Akiyama, A. Alberdi, W. Alef, K. Asada, R. Azulay, A.-K. Bacsko, D. Ball, M. Baloković, J. Barrett, and et al., *The Astrophysical Journal Letters* **875**, L1 (2019).
- [4] W. Israel, *Commun. Math. Phys.* **8**, 245 (1968).
- [5] B. Carter, *Phys. Rev. Lett.* **26**, 331 (1971).
- [6] L. Hui and A. Nicolis, *Phys. Rev. Lett.* **110**, 241104 (2013), arXiv:1202.1296 [hep-th].
- [7] A. A. H. Graham and R. Jha, *Phys. Rev. D* **89**, 084056 (2014), arXiv:1401.8203 [gr-qc].
- [8] T. P. Sotiriou, *Class. Quant. Grav.* **32**, 214002 (2015), arXiv:1505.00248 [gr-qc].
- [9] O. J. Tattersall, P. G. Ferreira, and M. Lagos, *Phys. Rev. D* **97**, 084005 (2018), arXiv:1802.08606 [gr-qc].
- [10] C. A. R. Herdeiro and E. Radu, *Phys. Rev. Lett.* **112**, 221101 (2014), arXiv:1403.2757 [gr-qc].
- [11] T. Clifton, P. G. Ferreira, A. Padilla, and C. Skordis, *Phys. Rept.* **513**, 1 (2012), arXiv:1106.2476 [astro-ph.CO].
- [12] E. G. Adelberger, B. R. Heckel, and A. E. Nelson, *Ann. Rev. Nucl. Part. Sci.* **53**, 77 (2003), arXiv:hep-ph/0307284 [hep-ph].
- [13] V. Cardoso, S. Chakrabarti, P. Pani, E. Berti, and L. Gualtieri, *Phys. Rev. Lett.* **107**, 241101 (2011), arXiv:1109.6021 [gr-qc].
- [14] J. Barranco, A. Bernal, J. C. Degollado, A. Diez-Tejedor, M. Megevand, M. Alcubierre, D. Nunez, and O. Sarbach, *Phys. Rev. D* **84**, 083008 (2011), arXiv:1108.0931 [gr-qc].
- [15] V. Cardoso and L. Gualtieri, *Class. Quant. Grav.* **33**, 174001 (2016), arXiv:1607.03133 [gr-qc].
- [16] R. Brito, V. Cardoso, and P. Pani, *Lect. Notes Phys.* **906**, pp.1 (2015), arXiv:1501.06570 [gr-qc].
- [17] T. Jacobson, *Phys. Rev. Lett.* **83**, 2699 (1999), arXiv:astro-ph/9905303 [astro-ph].
- [18] G. W. Horndeski, *International Journal of Theoretical Physics* **10**, 363 (1974).
- [19] C. Deffayet, G. Esposito-Farese, and A. Vikman, *Phys. Rev. D* **79**, 084003 (2009), arXiv:0901.1314 [hep-th].
- [20] M. S. Turner, *Phys. Rev. D* **28**, 1243 (1983).
- [21] W. Hu, R. Barkana, and A. Gruzinov, *Phys. Rev. Lett.* **85**, 1158 (2000), arXiv:astro-ph/0003365 [astro-ph].
- [22] L. Amendola and R. Barbieri, *Phys. Lett.* **B642**, 192 (2006), arXiv:hep-ph/0509257 [hep-ph].
- [23] D. J. E. Marsh and P. G. Ferreira, *Phys. Rev. D* **82**, 103528 (2010), arXiv:1009.3501 [hep-ph].
- [24] T. Regge and J. A. Wheeler, *Phys. Rev.* **108**, 1063 (1957).
- [25] S. Chandrasekhar, *The Mathematical Theory of Black Holes*, Oxford classic texts in the physical sciences (Clarendon Press, 1998).
- [26] P. P. Fiziev, *Class. Quant. Grav.* **23**, 2447 (2006), arXiv:gr-qc/0509123 [gr-qc].
- [27] P. P. Fiziev, (2006), arXiv:gr-qc/0603003 [gr-qc].
- [28] V. B. Bezerra, H. S. Vieira, and A. A. Costa, *Class. Quant. Grav.* **31**, 045003 (2014), arXiv:1312.4823 [gr-qc].
- [29] H. S. Vieira, V. B. Bezerra, and C. R. Muniz, *Annals Phys.* **350**, 14 (2014), arXiv:1401.5397 [gr-qc].
- [30] L. Hui, D. Kabat, X. Li, L. Santoni, and S. S. C. Wong, (2019), (to appear) [astro-ph.CO].
- [31] J. Alexandre and K. Clough, *Phys. Rev. D* **98**, 043004 (2018), arXiv:1805.01874 [hep-ph].
- [32] H. Witek, V. Cardoso, A. Ishibashi, and U. Sperhake, *Phys. Rev. D* **87**, 043513 (2013), arXiv:1212.0551 [gr-qc].
- [33] K. Clough, P. Figueras, H. Finkel, M. Kunesch, E. A. Lim, and S. Tunyasuvunakool, *Class. Quant. Grav.* **32**, 245011 (2015), [Class. Quant. Grav.32,24(2015)], arXiv:1503.03436 [gr-qc].
- [34] M. Adams, P. Colella, D. T. Graves, J. N. Johnson, N. D. Keen, T. J. Ligocki, D. F. Martin, P. W. McCorquodale, D. Modiano, P. O. Schwartz, T. D. Sternberg, and B. Straalen, .
- [35] K. Clough, T. Dietrich, and J. C. Niemeyer, *Phys. Rev. D* **98**, 083020 (2018), arXiv:1808.04668 [gr-qc].
- [36] J. M. Bowen and J. W. York, *Phys. Rev. D* **21**, 2047 (1980).
- [37] M. W. Horbatsch and C. P. Burgess, *JCAP* **1205**, 010 (2012), arXiv:1111.4009 [gr-qc].
- [38] L. K. Wong, A.-C. Davis, and R. Gregory, (2019), arXiv:1903.07080 [hep-th].
- [39] E. Berti, V. Cardoso, L. Gualtieri, M. Horbatsch, and U. Sperhake, *Phys. Rev. D* **87**, 124020 (2013), arXiv:1304.2836 [gr-qc].
- [40] D. Blas, D. L. Nacir, and S. Sibiryakov, *Phys. Rev. Lett.* **118**, 261102 (2017), arXiv:1612.06789 [hep-ph].
- [41] M. C. Ferreira, C. F. B. Macedo, and V. Cardoso, *Phys. Rev. D* **96**, 083017 (2017), arXiv:1710.00830 [gr-qc].
- [42] M. Rozner, E. Grishin, Y. B. Ginat, A. P. Igoshev, and V. Desjacques, (2019), arXiv:1904.01958 [astro-ph.CO].